Complex recruitment dynamics with Doppler-like effects caused by shifts and cycles in age-at-recruitment

K.N.I. Bell

Abstract: Even with constant production (N_0) and constant time-specific mortality (Z, daily), recruitment can vary greatly. A new variable-lag phenomenon modelled here generates temporal variation in recruitment from temporal shifts in age-at-recruitment (AAR; here synonymous with stage duration). The phenomenon is due to two components, one being analogous to the Doppler effect and the other an interaction of dAAR/dt with Z, and is distinct from those identified in previous contributions not focusing on temporal structure. Recruitment can be predicted from N_0, Z, and AAR, using either numerical simulation or, in many cases, the modified Doppler equation given here. Seasonal recruitment cycles predicted for a sinusoidal AAR function fitted to natural data, with constant larval production and constant Z (varied among, not within, model runs), were strongly peaked with a difference of 20% between maximum and minimum recruitments at $Z = 0$, to a difference of 2000% at $Z \approx 0.2$. The model gives indirect access to parameters difficult to measure in the field: if temporal variation is adequately described in two of the three input variables (N_0, Z, or AAR), differences (residuals) between predicted and observed recruitment can indicate an unaccounted pattern in the unknown.

Résumé : Même lorsque la production (N_0) et la mortalité spécifique du temps (Z, quotidienne) sont constantes, le recrutement peut varier considérablement. Un nouveau phénomène de décalage variable modélisé ici produit une variation temporelle du recrutement à partir de changements temporels touchant l'âge au recrutement (AAR; ici synonyme de durée du stade). Le phénomène est dû à deux composantes, une qui est analogue à l'effet Doppler, et est distincte des contributions antérieures qui ne sont pas centrées sur la structure temporelle. On peut prévoir le recrutement à partir de N_0, Z et AAR en utilisant soit une simulation numérique ou, dans nombre de cas, l'équation de Doppler modifiée présentée ici. Les cycles de recrutement saisonniers prévus pour une fonction AAR ajustée aux données naturelles, avec une production larvaire constante et un Z constant (qui variait d'un passage du modèle à l'autre, mais non dans un même passage), présentaient des pics prononcés, comportant des différences entre les recrutements maximum et minimum allant de 20 % à $Z = 0$, jusqu'à 2000 % à $Z \approx 0{,}2$. Le modèle donne indirectement accès à des paramètres difficiles à mesurer sur le terrain : si la variation temporelle est décrite adéquatement dans deux des trois variables d'entrée (N_0, Z ou AR), les différences (résidus) entre le recrutement prévu et le recrutement observé peuvent indiquer une caractéristique inexpliquée dans la variable inconnue.
[Traduit par la Rédaction]

Introduction

Although Roughgarden et al. (1988) comment that erratic fluctuations in abundance of exploited species have long standing as a topic of human interest, regular fluctuations, particularly those seen in species with seasonal variation in recruitment, are of equal interest. Explanations for recruitment variation over time are often sought in terms of variations in larval production (Robertson et al 1988; Robertson 1990), mortality (Houde 1987; Pepin 1989, 1991; Hoenig et al. 1990), or abiotic factors (Peterman and Bradford 1987). It is well known that increased stage duration (Houde 1987) or age-at-recruitment (AAR) can reduce recruitment, as is evident from the equation $N_t = N_0 e^{-Zt}$. It is also evident that, because t (in this context synonymous with AAR) is in the exponent, symmetrically increasing within-cohort variance of t increases recruitment because the increase in survival of that part of the cohort that experiences reduced AAR exceeds the reduction in survival of that part of the cohort that experiences increased AAR.

New to the present work is the link between a cycle or pattern of temporal change in AAR with a temporal pattern in recruitment. Profound changes in recruitment can result from temporal shifts in AAR, and acknowledging these may help to correctly identify other sources of recruitment variation.

Temporal change in AAR (i.e., a nonzero first derivative of AAR with respect to time, dAAR/dt) occurs naturally in *Sicydium* spp. (Bell et al. 1995), and has plausible origins in, for example, growth rate response to seasonal variations of temperature, food supply, wind, and mixing and may also respond to varying costs and benefits that an individual experiences by recruiting (Werner and Gilliam 1984). Growth rate and AAR are linked of course, but the dynamics that link them to recruitment success require exploration in terms of time, as AAR, "stage duration" as used by Houde (1987), or "postlarval duration" (Wellington and Victor 1992), etc. The terms and abbreviations important to this paper are summarized in Table 1.

Temporal changes in AAR will have unavoidable, and often

Received July 25, 1996. Accepted December 10, 1996.
J13572

K.N.I. Bell.[1] Biology Department and Ocean Sciences Centre, Memorial University of Newfoundland, St. John's, NF A1B 3X9, Canada.

[1] Address for correspondence from August 1997 – August 1998: Hugh Kelly Fellow, J.L.B. Smith Inst. Ichthyology, Rhodes University, Private Bag 1015, Grahamstown, 6140 South Africa. e-mail: ihkb@giraffe.ru.ac.za

Table 1. Abbreviations, definitions, and notation.

Abbreviation	Description
Variables	
AAR	Age at recruitment, usually the number of days from hatch to recruitment, but this term could be applied to the duration of any stage (synonymously with stage duration as used by Houde 1987). "One AAR" (etc.) may also be used to identify a unit of time approximately equal to age-at-recruitment
AAR curve	AAR as a function of hatch date unless otherwise qualified
DOY	Day of the year, numbered 0–365 (e.g., DOY = 0.5 means 12 noon on Jan. 1)
RDOY	Day of the year transformed to angular measure, usually radians (multiply DOY by $2\pi/365$)
LBBL	Barrels (≈80 L) of fish landed by the artisanal fishery for *Sicydium* spp. at Layou River in Dominica, used as an index of recruitment intensity
Subscripts	
hatch	Indicating that the main variable (e.g., DOY_{hatch}, $RDOY_{hatch}$) is taken at hatch (or estimated from regression against hatch date)
rcrt	Indicating that the main variable (e.g., DOY_{rcrt}, $RDOY_{rcrt}$) is taken at recruitment (or estimated from regression against recruitment date)
Labels and terms for models	
HDR model	Hatch date referenced model, i.e., the AAR function reflects expectation of AAR for given hatch date (this is the model used here in simulations)
RDR model	Recruit date referenced model, i.e., the AAR function reflects expectation of AAR for given recruitment date (no simulations done here with this model)
Absolute slopes	($\lvert dAAR/dt \rvert$); the absolute value of the slope of a curve. If, in an AAR curve, this exceeds 1.0 there will be bimodal age distributions in a HDR model or recruitment shadows in a RDR model
Cardinal points	The four cardinal points on the AAR function are extremes (minimum and maximum AAR) and nodes (the most positive and the most negative derivatives, $dAAR/dt$). These are useful for predicting phasing of the recruitment peaks and troughs under conditions of either high (using AAR) or low (using $dAAR/dt$) time-specific mortality
Surface	Recruitment surface, hatch surface; on model graphs, the locations where larvae hatch or recruit
Terms in periodic regression (Bliss 1958; Batschelet 1981; Bell et al. 1995)	
Mesor	The expected mean value of one full cycle of a periodic function. In estimation of the regression it functions like an intercept
Amplitude	The absolute distance from the mesor to the highest or lowest points in a periodic function
Others	
t	Time (in days)
S	Survival, time-specific (in units·day^{-1}); $= (N_t/N_0)^{1/t}$
M	Mortality, time-specific (in units·day^{-1}); $= 1 - (N_t/N_0)^{1/t}$
S_{cum}	Survival, cumulative; $= S^t$
M_{cum}	Mortality, cumulative; $= 1 - S^t$ (note that M^t is nonsensical)
N_0	Numbers entering a stage (e.g., numbers hatching)
N_t	Numbers completing a stage (e.g., numbers recruiting)
Z	Instantaneous total mortality ($= -\ln S$ (Ricker 1975), in units·day^{-1}). Outside the fisheries context the expression e^{-Z} could equate with e^r
Cohort	A group of individuals having in common some identified feature of interest, such as the same hatch or recruit date, according to context
For Doppler equations	
F_s, F_p	Frequency of a signal as emitted by source (F_s), and as perceived (F_p) by observer; for light or sound this is Hertz or cycles per unit time; for recruitment this is individuals per unit time
POSITION	Distance (or time) from source to observer
C	Rate of propagation of a signal between the source and observer

Note: Many names and labels use acronymic combinations of letters; therefore, multiplication is explicitly indicated by a times sign or use of brackets where it is otherwise ambiguous.

large, consequences for recruitment dynamics. These consequences arise from both *i* a variable-lag effect and *ii* its interaction with time-specific mortality. The variable-lag effect seems to be the first demonstration of a population-dynamic example of the Doppler effect. The combined action of *i* and *ii* can be modelled either by numerical simulation (which requires very few assumptions) or by the modified Doppler equation. Although the explorations below assume constancy over time of both reproductive effort and time-specific mortality rates, any variation in these would contribute to the final pattern; a potentially useful implication is that this affords an approach to investigating them indirectly. The existence of

Fig. 1. Seasonal variations in AAR (as function of hatch date and recruitment date) and recruitment for *S. punctatum* in Dominica, W.I. Panels A, C, and E are positioned so that the same dates are vertically aligned. Dates are indicated as day numbers beginning with January 1, 1989. Curves are least-squares periodic regressions given in Table 2 (all significant). (A) AAR vs. hatch date. Inclination of groups of points is because samples were collected at recruitment, not hatch, and $x_i + y_i$ = hatch date + AAR = collection date. (C) AAR vs. recruitment date. (E) Recruitment, in units of barrels (LBBL, ≈80 L) as indicated by the fishery at Layou river. Because periodic regression is uncommon I have presented two types of plots for clarity: "flat" (A, C, and E) and "cylindrical" (B, D, and F); the *x* axes for the cylindrical plots are DOY, first corrected by the lag (fitted rotation, worth 1 df), then converted to a standard (radians or degrees) angular scale, and finally converted to a cosine. Broken horizontal lines relate the mesor and amplitude of periodic regressions to normal regression on transformed variables.

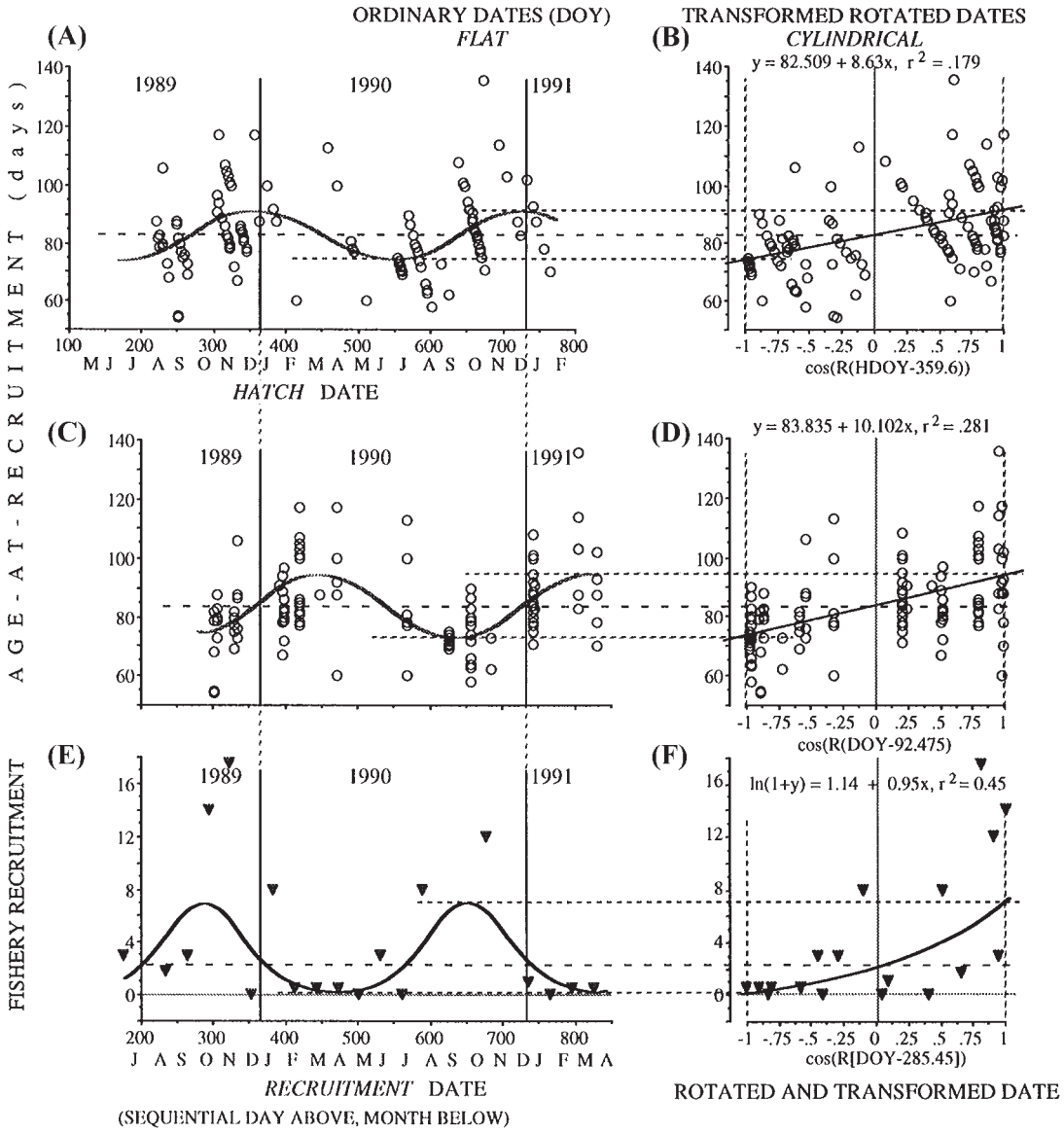

seasonal peaks in recruitment and their link with a seasonal variation in AAR have implications for the evolution of seasonal bias in reproduction.

In their discussion of recruitment, Roughgarden et al. (1988) recognised not only the complexities of two-phase (benthic–pelagic) life cycles, but also, implicitly, the value of using a natural change in niche and habitat (settlement) as a recruitment definition. Settlement is the outcome of a biological decision (Werner and Gilliam 1984) that may be thought to integrate many factors impinging on recruitment and fitness. Recruitment for *Sicydium punctatum* refers to the migration of postlarvae from the sea into freshwater, and this migration coincides with settlement and also a directed fishery. Seasonally, numbers of recruiting *S. punctatum* in Dominica, West Indies, vary from near nil to spectacular surplus. The temporal variation in AAR and recruitment provided the example for this study, and the temporal range in AAR was the basis for the input to simulations.

Although Bell et al. (1995) showed the first example of seasonally structured variation directly measured in AAR (Fig. 1, Table 2), it was not unexpected because seasonal growth rate variations had previously been shown and even

Table 2. Regression equations describing seasonal variations in AAR (age-at-recruitment) with respect to (A) hatch dates, (B) recruitment dates, and (C) fishery yield (reported as barrels, LBBL, ≈80 L) as an index of recruitment, with respect to recruitment dates (illustrated in Fig. 1).

(A) *Sicydium punctatum* AAR by hatch date			
$AAR_{hatch} = Int + \beta_1 sin(RDOY_{hatch}) + \beta_2 cos(RDOY_{hatch})$	r^2	*n*	*p*
(*i*) $AAR_{hatch} = 82.5 - 0.794 sinRDOY_h + 8.593 cosRDOY_h$ $p = 0.7462$ $p = 0.0001$ peak at DOY 359.6, amplitude = 8.63	0.179	117	0.0001
which can be rewritten as			
(*ii*) $AAR_{hatch} = 82.5 + 8.63 cos(2\pi(DOY_{hatch} - 359.6)/365)$			
which closely approximates the (more conservative) function applied in simulation:			
(*iii*) $AAR_{hatch} = 81.3 + 6.4 cos(2\pi(DOY_{hatch} - 0)/365)$ peak at DOY 365 or DOY 0, amplitude = 6.4			
(B) *Sicydium punctatum* AAR by recruitment date			
$AAR_{rcrt} = Int + \beta_1 sin(RDOY_{rcrt}) + \beta_2 cos(RDOY_{rcrt})$	r^2	*n*	*p*
$AAR_{rcrt} = 83.835 + 10.1 sinRDOY_{rcrt} - 0.21 cosRDOY_{rcrt}$ $p = 0.0001$ $p = 0.9243$ peak April 2, amplitude 10.102	0.28	117	0.0001
(C) *S. punctatum* recruitment (LBBL) by recruitment date			
$\ln(1+LBBL) = Int + \beta_1 sin(RDOY_{rcrt}) + \beta_2 cos(RDOY_{rcrt})$	r^2	*n*	*p*
$\ln(1+LBBL) = 1.13 - 0.93 sinRDOY_{rcrt} + 0.19 cosRDOY_{rcrt}$ $p = 0.0024$ $p = 0.4541$ peak at day 285.4 (Oct. 12)	0.45	19	0.0079

Note: See Table 1 for abbreviations. These data were collected in Dominica, W.I., 1989–1991. Regression A (*iii*) was used as simulation input; the expressions "– 359.6" and "– 0" are nearly the same thing for a 365-unit cycle. A minor (<5%) component of the goby-fry fishery consists of species other than *S. punctatum*.

incorporated into estimation of the von Bertalanffy growth function (Pitcher and MacDonald 1973; Pauly 1985), and the estimation of *Z* from catch curves (Pauly 1990). Also, seasonality exists in environmental variables, and there is within-cohort, individual variation in AAR (Victor 1982, 1984, 1986*a*, 1986*b*; Chambers and Leggett 1987; Wellington and Victor 1989, 1992; Cowen 1991; McCormick 1994); these also support the possibility of variation in AAR over time.Therefore, it is likely that many taxa (of fish particularly, but also of insects and plants) may show some seasonally structured variation in AAR.

Temporal change in AAR affects recruitment in unexpected ways, so the purpose here is to develop a framework to understand and predict these. If factors such as reproduction or survival vary over time they will also contribute to recruitment variation, but they are held constant in explorations below to isolate the effects of changes in AAR.

In this paper, I show how temporal AAR variation can influence recruitment. The arguments are mathematical rather than biological and, therefore, are not restricted to fish. I model the mechanisms graphically, showing qualitative differences that depend on levels of variation in AAR and also on the life-history stage where the AAR is assumed to be set or ordained. I show graphically the similarity of one model (hatch-date referenced (HDR), which assumes that AAR is set at hatch) to the Doppler effect. I use numerical simulations to explore the dynamics of this model using various functions, including AAR data for *S. punctatum*, as input to the model. I show that the phenomenon by which temporal pattern in AAR generates temporal pattern in recruitment can also be modelled by modified Doppler equations. Sinusoidal variation is the simplest structure for cycles (cf. Pitcher and MacDonald 1973; Pauly 1985) and, therefore, a good starting point for describing temporal changes in AAR, although the prediction methods are not constrained to sinusoidal variations. The dynamics apply to numbers entering and exiting any stage of variable duration, so where I use "hatch" and "recruitment" it can be read as "entering" and "exiting" a stage.

Theory and models

The theoretical basis for a relationship of changing AAR to changing recruitment is twofold, arising out of (*i*) the derivative of AAR with respect to time, or dAAR/d*t*, and (*ii*) the value of AAR. (*i*) The temporal spacing of hatch cohorts is disrupted (see Figs. 2–4) by changing AAR: temporal spacing at recruitment (apparent frequency) differs from original spacing at hatch (source frequency). This is strictly due to dAAR/d*t* and is analogous to the Doppler effect, which is the alteration of perceived signal frequencies due to displacement of either the source or observer during either the production or reception of the signal. Doppler algebra is given in the section on HDR models. (*ii*) A constant time-specific mortality rate (*Z*) compounded over varying periods of time gives exponentially varying cumulative or total mortality, so that temporal changes in AAR can cause much greater temporal changes in recruitment. This arises from the familiar equation:

$$(1) \qquad N_t = N_0 e^{-Z(t-0)}$$

where *N* represents cohort size, $t - 0$ is the number of time units (equivalent to AAR) that separate N_0 and N_t, and *Z* is the natural

Fig. 2. (A) Recruitment dynamics, HDR model (hatch-date referenced), moderate slopes only (all $|dAAR/dt| \leq 1.0$; see text). This is the situation used in simulations. The x axis represents one annual cycle. Recruitment over the period AB (arbitrarily chosen) results from larval production over period GH. By definition, the number of days to recruitment declines by 1 each day of an individual's life, so slopes of figure eqs. 2 and 3 are –1. Rate of recruitment (recruits arriving per unit time) is more intense over the period AB than is hatching (per unit time) over the corresponding period (GH), but the opposite occurs in other seasons. Note that vertically moving the AAR curve changes the interval between hatch and recruit times, but the extent of convergence or divergence of recruitment is affected only by the slope of the curve. (B) Doppler analogy: a stellar example fitting the HDR model with a sinusoidal function would be a binary star system: light from the bright star would be red-shifted (longer wavelength, lower frequency) when receding and blue-shifted when approaching. The distortion of a source frequency by relative motion of the source and observer is analogous to the distortion of rate of larval production by temporal shift in the lag from hatch to recruitment (or change in AAR). The speed of light is indicated by a 45° line (units distance/time or light-year/year); similarly, the speed of transmission of a larval pulse is –1 (units day remaining/day elapsed).

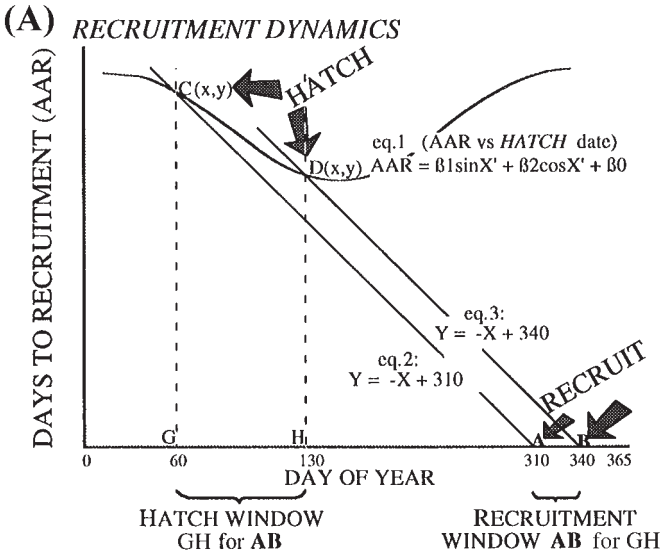

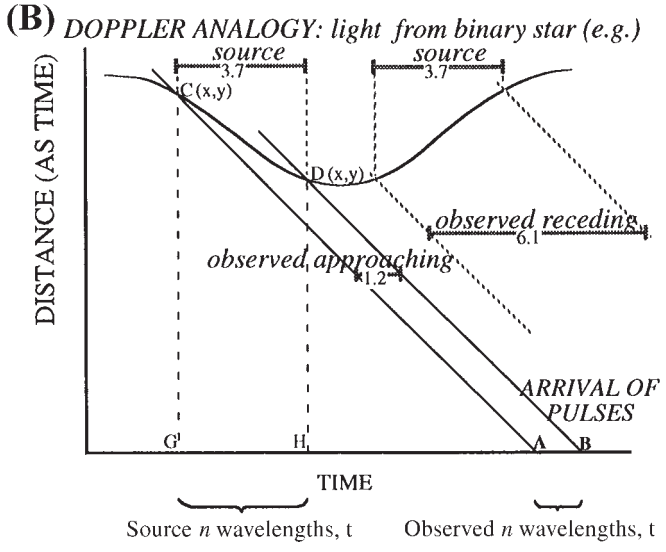

Fig. 3. Recruitment dynamics, HDR model (hatch-date referenced), with high slopes (extremes of $|dAAR/dt| > 1.0$; see text and previous figure legend). Where $dAAR/dt < -1$, recruits show bimodal age distribution at some times. The mechanics are similar to the previous example, except that because of the high negative slope (i.e., $dAAR/dt < -1$) it is possible to have multiple intersections of the AAR curve (figure eq. 1) with larval trajectories (figure eqs. 2, 3, etc.), and this causes the hatch window corresponding to the recruitment window AB to be split (GI and JH), giving rise to bimodal age distribution in recruits near A. Larvae hatching in the interval IJ (within GH) recruit prior to time A (hatch order disrupted), and recruitment is in precisely the reverse order of hatches when $dAAR/dt < -1$.

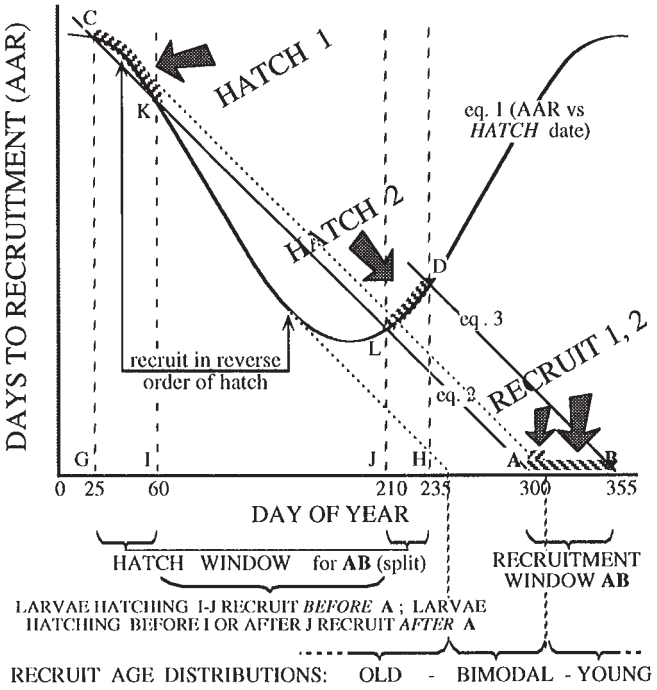

logarithm of survival ($S = e^{-Z}$, $Z = -\ln S$) with the sign changed (Ricker 1975). Outside the fisheries context the expression e^{-Z} could equate with e^{r}. N_0 and N_t are the beginning and end of a period represented by AAR or stage duration (and may be used for numbers at an egg, larval, juvenile or any other stage, provided that N_0 precedes N_t).

To conceptualize these dynamics, assume that AAR is substantially determined at the date of occurrence of some major event in the early life history. Although any dates (e.g., hatch, recruitment) in the hatch to recruitment period may have some influence on AAR, the beginning (hatch date) allows the most tractable models, and there is at present little basis on which to prefer other models. Therefore, this paper uses HDR models for simulations, but for contrast I shall also describe recruitment date referenced (RDR) models. The results of these two are qualitatively quite different. HDR models are more plausible than RDR models because the hatch date (predictor) precedes the recruitment date (predicted), instead of the other way around. To illustrate the main qualitative differences in the range of possibilities, three basic graphic models are presented: HDR models with AAR curves having maximum absolute slopes ($|dAAR/dt|$) less than 1.0 (Fig. 2) or exceeding

Fig. 4. Recruitment dynamics, RDR model (recruitment-date referenced), with extremes of $|dAAR/dt| > 1.0$. (RDR models are not applied in the simulations.) If AAR is thought of as being determined at recruitment date instead of hatch date, qualitatively different dynamics are generated if maximum slope of the AAR curve also exceeds 1. Larvae hatched in interval GI gain age at one day per day, until intersection with the AAR curve, which now acts as a recruitment surface; they recruit in interval AB. However, recruitment is zero under segments of the AAR curve from above B, where maximum slope first exceeds 1, to the point where the next larval trajectory (line having slope = 1) passing the AAR curve above B intersects with the AAR curve (above J). Thus, while production during GI is recruited over the similar interval AB, the point marked I is the hatch date where, suddenly, time to intersection with the AAR curve becomes very long, so there is no recruitment between B and J (shaded). Larvae hatched between I and K recruit between J and H, a narrower interval, giving (assuming $S = 1.0$) a rise in recruitment rate not due to any change in larval ($stage_0$) production rate.

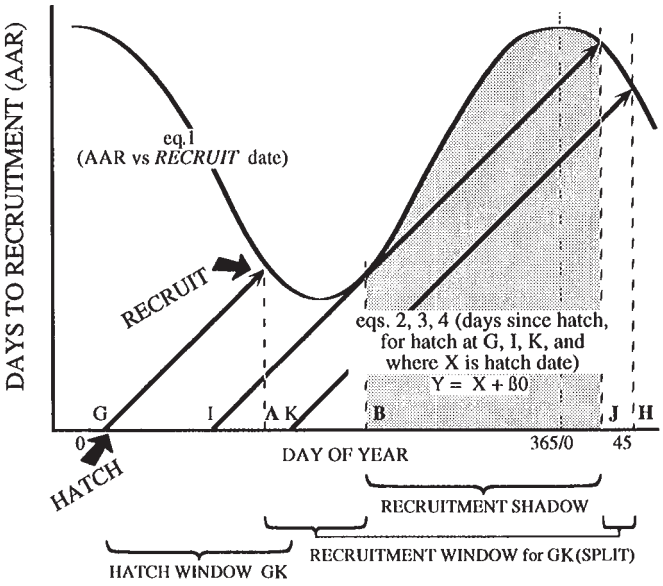

1.0 (Fig. 3) and an RDR model with AAR curve having maximum absolute slope exceeding 1.0 (Fig. 4).

The main components of the graphic models are hatch surfaces and recruitment surfaces. Larvae originate on the hatch surfaces and, with accumulation of age, progress on a 1:1 line (negative in the HDR model, positive in the RDR model) toward the recruitment surface. The first intersection of a larval trajectory with a recruitment surface indicates by definition a recruitment event, but any intersection of a larval trajectory after hatch with the hatch surface has no consequence (recruitment surfaces are defined as opaque, hatch surfaces transparent).

Hatch date referenced AAR (HDR model)

In the HDR model, a hatch event is represented (Fig. 2) on the AAR curve by x_i (date) and y_i (the ordained AAR for that hatch date, AAR_{hatch}). All (x_i, y_i) on the graph denote (date, (AAR – age)); the AAR curve is consistent with this because a hatching larva has age = 0. The function for AAR_{hatch} can be readily estimated from data by periodic regression (Bliss 1958; Batschelet 1981; Bell et al 1995) of AAR against hatch date. A line with slope –1 originating on the AAR curve represents the (date, (AAR – age)) trajectory of a larva, and it will intersect with the x axis ($y = 0$) at the recruitment date. These lines can be used to graphically locate the hatching interval corresponding with any recruitment interval, or vice versa. Figure 2A shows the simplest situation: for an AAR_{hatch} curve with $-1 <$ slopes < 1 (this is the model used with *S. punctatum* data for simulations below). The spacing of larvae at recruitment can differ markedly from that at hatch (Fig. 2).

The Doppler effect analogy (for the HDR model) The model describing recruitment variation resulting from varying AAR (Fig. 2A) is analogous to the Doppler effect (Doppler 1842), named for its discoverer. The Doppler principle explains how a frequency shift (e.g., in light or sound) is generated by relative motion of source and observer in space (Fig. 2B). The principle is important in astronomy for estimating stellar motion from shifts in absorption lines. The principle can be expressed as

$$(2) \quad F_p = F_s(1 - (\mathrm{dPOSITION}/\mathrm{d}t)/C)$$

where F_s, the frequency generated at source, is perceived as F_p at some distant point according to the relative radial motion dPOSITION/dt (negative if source approaching, positive if receding) compared with C, the speed of signal propagation (Otten 1992). POSITION is the distance (or the time required for the signal to traverse that distance at velocity C) between the signal source and the observation point where it is perceived. The variate POSITION is most conveniently expressed in units of time separating the source and observer given the velocity C (for example, light-years); the time coordinate for the arriving signal is simply $t_p = t_s +$ POSITION. I'll ignore the correction for relativity. A similar effect could occur if the speed of transmission changes (for sound, this would occur if air density changed) or if the signal takes a longer route.

A changing AAR is analogous to changing position of a signal emitter relative to an observer, because it varies the time until recruitment. Like a Doppler effect, the perceived (recruitment) frequency differs from the hatching frequency only when AAR (or POSITION) is changing; when $dAAR/dt = 0$ the frequency of recruitment reflects the frequency of hatching.

The Doppler equation can be used to calculate recruitment by treating as frequencies the rates of larval production (F_s) and subsequent recruitment (F_p), and taking C to be unity (absolute value of d(age)/dt, or the slope of signal trajectory in Fig. 2). To incorporate mortality, the Doppler formula as used for light or sound requires extension by multiplying F_p (as obtained above) by time-specific survival exponentiated to the time over which the fish (etc.) is exposed to such mortality:

$$(3) \quad \mathrm{Recruitment} = F_s\,(1 - (\mathrm{dPOSITION}/\mathrm{d}t)/C)S^{AAR}$$

and of course the date of recruitment is obtained by adding AAR to the hatch date. Where mortality is not constant over time, the cumulative product of the daily survivals for the hatch to recruitment period ($S_0 \times S_1 \times ... \times S_{recruitdate-1}$) should be used to replace the expression S^{AAR} (eq. 3).

The recruitment equation based on the Doppler equation gives virtually the same results as a numerical simulation model used below (the simulation results are slightly more

noisy because of recruitment-date overlaps and misses). However, results from the numerical simulations are relied on, because simulation does not assume a Doppler analogy. The simulation data illustrate the phenomenon and provide a basis to evaluate the predictions from the modified Doppler equation (eq. 3) and the analogy. It will be shown that the modified Doppler equation allows easier prediction of recruitment from temporal variations in AAR, provided that |dAAR/d*t*| is less than about 0.5.

Hatch date referenced AAR with rapid change (HDR + steep slope)

If the most negative slope of the AAR_{hatch} curve is lower than –1, some recruitment periods will correspond to two non-adjacent hatch intervals (Fig. 3). The consequence is a bimodal or discontinuous age distribution in the recruits in some parts of the cycle (although where recruit ages are potentially bimodal, mortality would affect the older cohort for a longer time and exponentially reduce its proportion). For a portion of the AAR curve with slope less than –1, recruitment order will be the reverse of hatching (Fig. 3). A special case would exist with any kind of AAR curve with slopes for some segment exactly equal to –1.0 for some time; convergence would be infinite, so that all larvae hatching (or individuals entering the stage of interest) on this segment would recruit (or complete the stage) at a single instant. In more complex functions, high dAAR/d*t* may be more commonly seen than in sinusoidal functions with the same overall range, and if so these recruitment dynamics may prevail during parts of the cycle.

Recruitment date referenced AAR with rapid change (RDR + steep slope)

A brief caveat is that AAR could be treated as a function of dates other than hatch date, and this could result in qualitative differences where AAR curves have slopes steeper than ±1. For example, I could view AAR as being determined at recruitment date instead of hatch date. The AAR function, AAR_{rcrt}, needed as a model input would then have been estimated from data by regressing AAR against recruitment date. In the RDR model's diagram (Fig. 4) the coordinates *x* and *y* denote date and age, respectively, and the vertical lines would then relate to the recruitment event. Positive 1:1 lines would lead from hatch at (*x*, 0) until recruitment, indicated by the intersection of these with the AAR_{rcrt} curve. The value of *Y* on this 1:1 line is (by definition in this model) equal to the larva's age at time *X* (whereas, in the HDR models, *Y* on a –1:1 line represented time remaining, at time *X*, until recruitment). Larvae cannot pass through the recruit surface, which here is the AAR_{rcrt} curve, but must recruit at first encounter. Because of this, where the AAR_{rcrt} curve has a slope >1, seasonal recruitment shadows can be formed and larvae recruiting after the shadow are then relatively old. In contrast, a HDR model could give bimodal age distributions in some seasons because of slopes less than –1. In the HDR model the recruitment surface was the *x* axis (which is flat and cannot project shadows on itself, so its opacity is of no consequence here) and the AAR_{hatch} curve was "transparent" so that hatched larvae are uninfluenced by re-encountering the curve after their own hatch dates; but in the RDR model the (opaque) recruitment surface is the AAR_{rcrt} curve, which can project shadows on itself because of its shape, and the hatch surface is flat and cannot be re-encountered.

Other models

Other geometric models could describe systems where AAR is determined at points partway through the hatch-to-recruitment period or other stage of interest. This matters if the early life-history points that best explain temporal pattern in AAR turn out to be intermediate between hatch and recruitment. A brief discussion is warranted because future work may be able to confirm this and identify the timing of the strongest influences on AAR.

For example, the "halfway" model: if the determination of AAR was deemed to occur halfway through the stage, the *x* axis would be both the hatch and the recruitment surface; the AAR function would be a half-AAR curve determined by regression of Y_i (= $0.5(AAR_i)$) against X_i (= recruit date – $0.5AAR_i$). A larval trajectory would begin on the *x*-axis (as in RDR model) and trace a positive 1:1 line until contact with the half-AAR function, would reflect off this and trace a negative (–1:1) line until intersecting with the *x*-axis (recruitment, as in the HDR model). Such a model would operate by predicting the AAR associated with the point of reflection. Because it has both negative and positive 1:1 lines for larval trajectories, it could produce both bimodal age distributions and recruitment shadows (in other words could produce the qualitative effects of both HDR and RDR models), but the half-AAR curve in the model would require real dAAR/d*t* of over 2.0 to yield the rate of change over 1.0 on the half-AAR curve that would be needed to produce these extreme effects.

Models referenced to intermediate points are more cumbersome to simulate, and at present not significantly more plausible, than the HDR models which occupy the bulk of this paper.

Methods

Source of data

The source of AAR data for simulation (numerical) and calculation (using modified Doppler equation) input is natural (Bell 1994; Bell et al. 1995), so the simulations are based on realistic variation. While it is likely that AAR might cycle in many species, it has been clearly demonstrated only in *S. punctatum* and *S. antillarum.* Sinusoidal variation in AAR, as seen in *Sicydium* spp. in Dominica, is one among many possible patterns of dynamically varying AAR.

Sicydium spp. are diadromous gobies, spawning in rivers and spending a postlarval period in the sea (see Fig. 2 and description of life cycle in Bell et al. 1995) before a migration back to and settlement in rivers (recruitment). Reproduction occurs year round, but recruitment is episodic and synchronized near the last lunar quarter (Bell et al. 1995). The highest recruitment (and fishery yield) occurs in the fall and the lowest in the spring. For *Sicydium* spp., recruitment coincides with settlement and is also the stage at which a fishery occurs, which was convenient because it provided quantitative estimates of recruitment. Thus, AAR for *Sicydium* spp. is like age-at-settlement or at metamorphosis, as used by other authors (Victor 1986*b*; Chambers and Leggett 1987; Radtke et al. 1988; Robertson et al. 1988; Wellington and Victor 1989; Cowen 1991; Markle et al. 1992; Robertson 1992; McCormick 1994). Biologically based definitions, because they recognise choices made by individuals, can suggest elements of the

decision process or constraints involved in recruitment (e.g., Bell et al. 1995, Fig. 7).

The periodic regression equation (Fig. 1, Table 2) presented for *S. punctatum* in Bell et al. (1995) is very close to the more conservative (lower amplitude) cyclic AAR function used here, which is

$$(4) \quad AAR = 81.3 + 6.4\cos(RDOY_{hatch} + 0),$$

where DOY is day of year, hatch denotes hatch date, RDOY is the DOY transformed to a cyclic variable in units of radians ($RDOY = DOY \times 2\pi/365$), and adding 0 indicates a nil phase lag with the calendar year (year as a circular variable). Periodic regression (Fig. 1, Table 2) is formally identical to linear regression of *Y* against a cosine transform of the *X* variable after adding a fitted lag (Bliss 1958; Batschelet 1981; Bell et al. 1995). The periodic regression of AAR against time of year is highly significant ($p = 0.0001$, $n = 191$). Although there is considerable variation among individuals at each date, the r^2s from equations based on individual data are conservative in the sense that they are much stronger predictors of the mean value for each sample date.

Modelling for the present purposes is best done using time or age, as, for example, stage duration (Houde 1987) or AAR. Conversions from size to age can sometimes give very misleading indications of relative ages because (*i*) there is an individual component to growth rates, and (*ii*) as seen in the *Sicydium* spp. data (Fig. 7 of Bell et al. 1995), the slope in an among-cohort regression of (using cohort means of) size-at-recruitment against AAR can be negative even though the size versus AAR slopes in within-cohort (using individual values) regressions are positive. Therefore, time should be estimated using a method (e.g., otoliths) that is independent of size.

Simulation using HDR models

Given an AAR-at-hatch curve (as in Fig. 2), the graphic methods make it possible to identify the production interval(s) corresponding to any chosen recruitment interval. Projecting temporal trends in recruitment using this method would be possible but tedious. Therefore, I further explore the HDR model using a numerical simulation program that incorporates the compounding effects of mortality over time on larvae hatching each modelled day. Although I show below that the modified Doppler equation can do the same thing in most circumstances, the numerical simulation method requires no assumptions other than the inputs to the simulation; this allows the results of numerical simulation to also serve as a test for the modified Doppler equation.

The simulations show the recruitment variation that can result from a situation where the following prevail: (*i*) AAR varies as a function of hatch date; (*ii*) larval output is held constant over time; and (*iii*) time-specific survival rates are held constant over time.

The simulation structure (Fig. 5) is based on each larva having an expected recruitment date, and the total number of recruits on a particular day being the sum of all larvae having that expected recruitment date, less mortalities. Cohort size at recruitment is given by eq. 1 or similar language:

$$(5) \quad N_t = N_0 e^{\ln(S)AAR}.$$

Of course, recruitment date is equal to hatch date plus AAR.

For most simulations (Fig. 5), I used an AAR function (eq. 4) with parameters close to those obtained from otolith data (Table 2) for *S. punctatum* (Bell et al. 1995). Scaled versions of this function, and a step function, were also used. For each day in the simulation, ages-at-recruitment, date of recruitment, and cumulative survival were calculated for a hatching cohort of 10^6 pseudoindividuals. Recruits were accumulated for each recruit date (day of year, treated as a cycle of period 365 and thence disregarding the year of recruitment) while the program cycled through an entire year of hatch dates. Fractional individuals were permitted. The simulation program wrote results to a file. Integer effects of date caused zeroes or approximate doubling when changing AARs passed whole numbers, so smoothing of plots was done by taking 28-day running means. The 28-day span was reasonable because recruitment of *S. punctatum* is episodic and lunar phased.

Results (simulations using the HDR model)

Simple change in age-at-recruitment

The simplest variation function used for AAR in a HDR model is a step function (Fig. 6). This is probably not natural, but it is instructive. The simplest case of this simplest function is where time-specific (daily) survival = 1.0 (Fig. 6, upper output panel): all cohorts have the same cumulative survival to recruitment, because $S^n = 1.0^n = 1.0$. Abrupt steplike increases in AAR are followed, after a delay approximating AAR (because that is how long it takes a signal to travel from hatch to recruitment), by abrupt decreases in recruitment (briefly to zero, because all recruitment has been postponed by the increase in AAR). The decrease is of a duration approximately equal to the change in AAR, so that a positive difference of 10 days in AAR results in a decrease in recruitment that lasts about 10 days. Restoration of previous AAR is just a change in the other direction: a 10-day decrease in AAR causes a (delayed) increase (briefly to twice the original level here because each recruit date is now collecting from two hatch dates) in recruitment, which lasts about 10 days (because that is for how long each recruit date collects from two hatch dates).

If we also add (Fig. 6, bottom panel) mortality ($S < 1.0$) compounded over AAR, cumulative survival will vary negatively and exponentially with AAR (eq. 5). The effects are similar to the zero-mortality (previous) situation, but recruitment is also diminished for the duration of the increase in AAR.

Thus, an abrupt change of AAR from one value to another affects recruitment (Fig. 6, bottom panel) in two ways: (*i*) transient spiky effects because the spacing of recruits is changed from their spacing at hatch and (*ii*) sustained effects (lower plateau in bottom panel) due to the compounding of mortality over the (changed) time represented by AAR. These two effects are both important but are less distinguishable when changes in AAR are gradual.

Sinusoidal change in age-at-recruitment

The sinusoidal AAR function used for the HDR simulations here approximates that found for AAR of *S. punctatum* (Fig. 1, Table 2). Day-to-day fluctuations in *S* or N_0 could be easily incorporated, but they play no role whatever in the simulations presented here.

Model runs over a range of daily survivals produce a range

Fig. 5. Flowchart for numerical simulation of effect of AAR variation on recruitment (numbers), showing steps taken by the program.

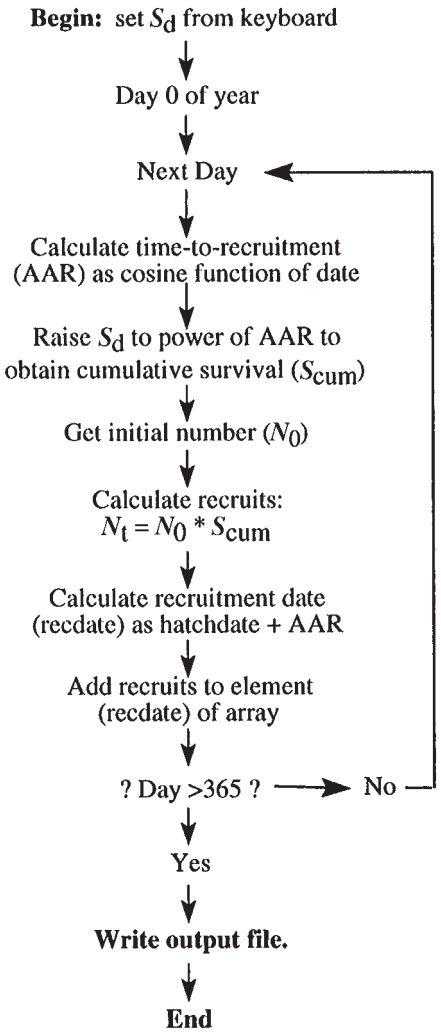

Fig. 6. Effects of abrupt changes in AAR (arbitrary, unnatural data). Reproduction is constant (10^6·day^{-1}) for this simulation. Upper graphs (A) show inputs to model: larval production and AAR over time. Lower graphs (B) show simulated recruitment patterns obtained with daily survival rates as noted on each graph.

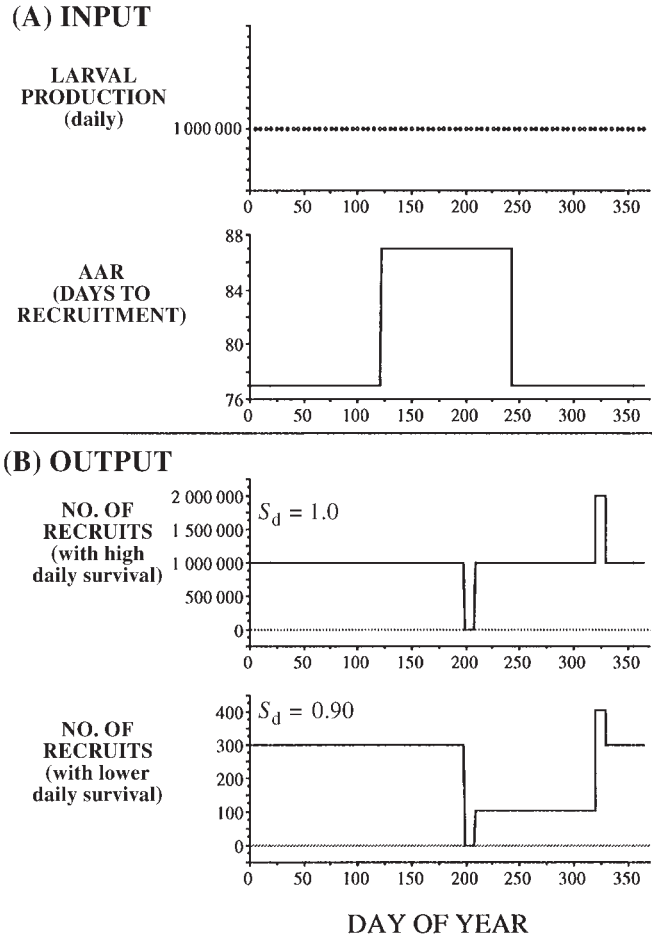

of recruitment profiles (Fig. 7). At $S = 1.0$ the variation (range/minimum) is 30%. The recruitment curve is a symmetrical hill with a maximum nearly coincident with the quickest AAR, but as will be seen this is a special case (mean AAR ≈ 0.25 × 365 days) and will not turn out to be a generality. At $S = 0.97$ the variation exceeds 50%, and the curve is losing its left–right symmetry as a trough of low recruitment begins to show on the left side. As S is reduced, the trough becomes a flat minimum that becomes lower and wider; the peak becomes relatively higher, narrower, and shifted to the right. At $S = 0.7$ the variation is 9600%, because recruitment is virtually zero during the winter and spring, and forms a narrow, relatively tall peak in the fall. (In field observations, minimum values may be low and erroneously interpreted as zeroes, which would inflate the apparent geometric variation, but the output of simulations is not subject to the same observational error.) Initially ($S = 1.0$) the peak is near day 180, the trough near day 0 (or 365). Progression of both of these is rapidly to the right as S decreases even minutely from 1.0, but the progression slows near $S = 0.90$, with little change down to $S = 0.60$.

Recruitment maxima and minima in scaled AAR curves

Scaling of the AAR function (Fig. 8) also affects the recruitment profile. I ran simulations using the naturally derived AAR function (eq. 4) multiplied by 2, 1, 0.5, and 0.25. This preserved the same variation relative to the mean. Because we saw in Fig. 7 that temporal locations of peaks and troughs changed little below $S = 0.90$, I plot only $S = 1.0$ and $S = 0.70$ to show recruitment patterns resulting under conditions of zero and substantial time-specific mortality.

The results show that, even though scaling preserves the seasonal phase of the AAR functions themselves, the seasonal phase of maxima or minima of recruitment are profoundly shifted by scaling. With doubled AARs (150–175 days to recruitment), curves are shifted to the right for both $S = 1.0$ and $S = 0.7$. With halved values the peak at $S = 1.0$ precedes the AAR minimum, while the $S = 0.70$ peak follows it by about 40 days. With quartered AARs, the $S = 1.0$ peak is further still to the left, and the $S = 0.70$ peak is only slightly later than the AAR minimum. As AAR is scaled downward, the recruitment peaks move to the left (occur earlier), and the tendency for mortality to distort the sinusoidal zero-mortality recruitment profile to a log-sinusoidal form is reduced.

Fig. 7. Simulation of effect of seasonally shifting AAR on recruitment. (A) Inputs to model are AAR (days to recruitment, natural data) and larval production (10^6·day^{-1}; constant), and time-specific survival input (constant over time), is noted on each output graph. (B) Output graphs show simulated recruitment profiles (28-day moving averages contribute a constant additional recruitment lag of ~14 days) obtained with each *S*. At daily $S = 1.0$, all variation is due to Doppler-like effects giving a recruitment peak near day 180, but the increasing role of mortality shifts the recruitment peak to the right, stabilizing where mortality effects dominate (in this example near day 265).

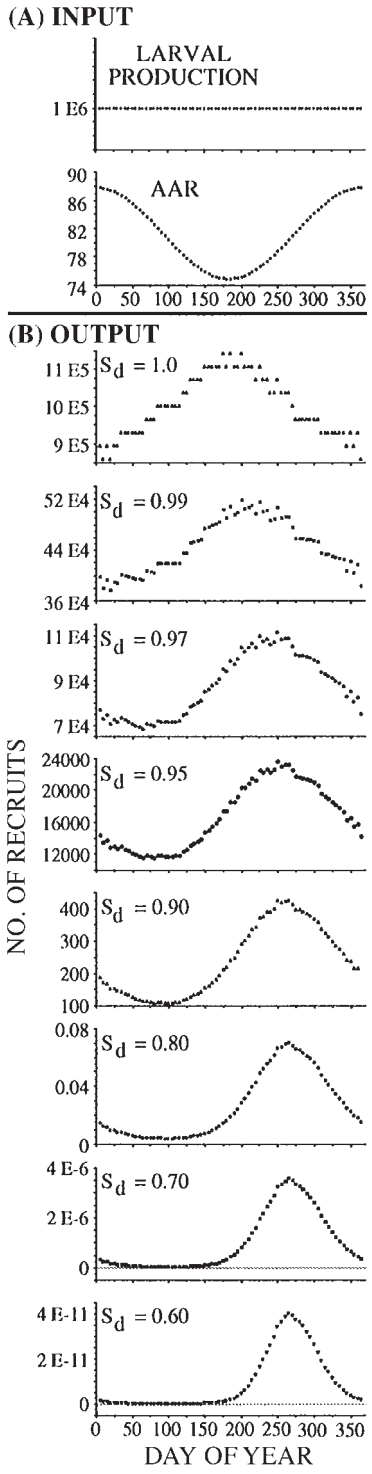

Discussion

Predicting timing or recruitment peaks from AAR curves

If we expected timing of peaks or valleys to always occur at the AAR minimum and maximum, the results will have seemed counterintuitive. At $S = 1.0$ ($Z = 0$) there is no difference in S_{cum} with varying AAR ($1^n = 1$). Here, the timing of recruitment peaks is purely determined by a Doppler-like effect, which causes convergence of multiple-day hatch cohorts on fewer recruitment days (Fig. 2) when AAR is decreasing. When AAR is increasing, divergence occurs instead. However, when time-specific mortality rates exceed 0 ($S < 1.0$), they interact with shifts in AAR to draw recruitment peaks away from their zero-mortality positions toward the recruitment dates corresponding to the lowest AAR, i.e., toward the date represented by the expression "hatch date + AAR" where hatch date is at the minimum AAR. With $S < 1.0$, fewer recruits result (eqs. 1, 5) from a slow-recruiting cohort (high AAR or t) than from a faster recruiting (shorter AAR) cohort; if recruitment occurs at a constant size then this would also be true for slower or faster growing cohorts. That this happens is nothing to do with size- or age-dependent mortality but is simply the result of accumulation of time-specific mortality, which is exponentially affected by AAR.

With diminishing S (increasing M and Z) the Doppler-like effect is increasingly swamped by variable survival. The seasonal recruitment profile thus shifts, as mortality increases from zero, from being Doppler dominated to being mortality dominated. This suggests how recruitment peak timing might be determined from the AAR_{hatch} curve.

On an AAR curve four "cardinal" points (Fig. 9) are useful for quick visual prediction of recruitment profile phasing. These are the extremes (maximum and minimum AAR) and the nodes (the most negative and the most positive derivatives, dAAR/dt). The AAR extremes are useful in prediction when mortality is high (e.g., $S \leq 0.7$), and the derivatives are useful when mortality is near zero ($S \approx 1.0$). On a sinusoidal curve, the cardinal points are equally spaced horizontally, but their projections (along larval trajectories or lines of slope = –1) onto the x axis fall on points which are less equally spaced with increasing amplitude of the AAR curve.

To predict recruitment phasing from the AAR curve, lines are drawn with slope –1 from the cardinal points (Table 1, Fig. 9). The intersections with the x axis (i.e., at $Y = 0$) mark the times of maximum and minimum recruitment, for either low mortality (lines from extremes of dAAR/dt) or high mortality (lines from extremes of AAR). At very low mortality rates ($S \approx 1.0$) the recruitment peak will be approximately one AAR after the most negative derivative, and the recruitment trough will be approximately one AAR after the most positive derivative. At higher mortalities (e.g., $S \approx 0.7$) the recruitment peak will approach a point approximately one AAR after the AAR minimum value, and the recruitment trough will approach a point approximately one AAR after the AAR maximum value. The transition from $S \approx 1.0$ to 0.7 (Fig. 7) shows joint influence, and cannot be predicted using simple geometry. In other kinds of curves or complex AAR cycles with multiple peaks and troughs, the same rules for prediction would apply.

Where the recruitment minima are wide troughs, the graphical

Fig. 8. Effect of scaling input AAR functions. Inputs and outputs represent all components of the equation $N_t = N_0 e^{-Z(t-0)}$. (A) Inputs to simulations are scaled naturally derived AAR functions, constant stage$_0$ production at $10^6 \cdot day^{-1}$, and time-specific survival as indicated on each row of output graphs. (B) Output of simulations (points are 28-day running means). From left to right: vertical groups of graphs represent simulations using AAR functions equal to 2×, 1×, 0.5×, and 0.25× the fitted values for *S. punctatum* in Dominica. From top down: input AAR in days, predicted recruitment assuming zero mortality ($S = 1.0$, $Z = 0$), and predicted recruitment assuming 30% mortality per day ($S = 0.7$, $Z = 0.36$).

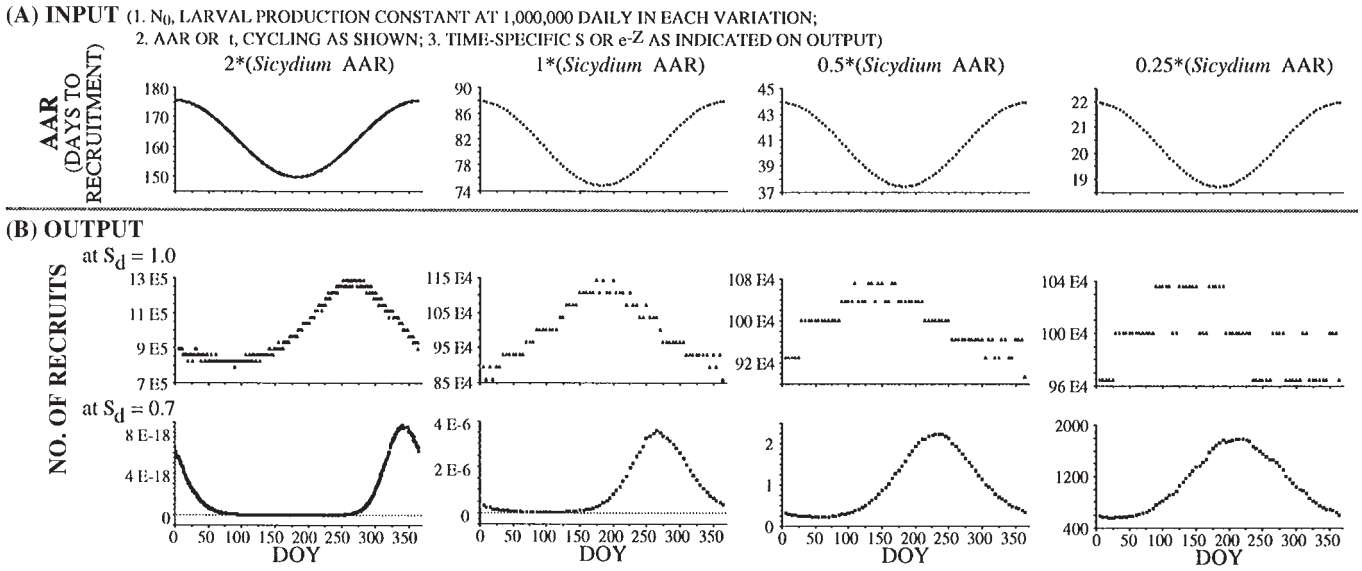

prediction method just described generally finds the center of the trough. A log *y* axis helps to show this. Relative variation (range/minimum) increases at higher mortality. The lower values occupy large ranges on logarithmic scales although they are (arithmetically) extremely close.

At low mortality rates and where the AAR function is sinusoidal, the maxima and minima of recruitment will be approximately one-half cycle apart because they depend on the derivatives (or nodes). At higher mortality this is less true, especially in sinusoidal curves with high d*AAR*/d*t*, because as amplitude of the curve increases, the maximum and minimum AAR approach the same diagonal (recruitment trajectory with slope of –1) so that the minimum recruitment can be very close to the maximum.

Effectiveness of the modified Doppler equation

The comparison of results (Fig. 10) of numerical simulation with those of the modified Doppler equation (eq. 3) are for an HDR model (i.e., assuming that AAR is determined at hatch). The results are virtually identical, supporting the analogy of this recruitment-dynamic phenomenon with the Doppler effect. The modified Doppler equation is more convenient than numerical simulation and can be set up in a spreadsheet to generate predictions, provided |d*AAR*/d*t*| stays smaller than 0.5. This caution is because, when |d*AAR*/d*t*| exceeds about 0.5, recruitment is underestimated, and furthermore when d*AAR*/d*t* > 1.0 (in the Doppler analogy this is where approaching velocity *V* exceeds *C*), a negative (nonsensical) number is calculated for F_p. When in doubt, results should be checked by numerical simulation.

Note that simulation explicitly deals with individuals, which then require summing over each recruitment time unit of interest (e.g., each day). In contrast, the modified Doppler equation treats hatch and recruitment as frequencies or rates, so that summing is inappropriate.

Conclusion and implications

Where AAR changes, simple arithmetic ordains that it will influence recruitment (N_t); the eventually realised recruitment variation is a summation of the effects (eqs. 1–3, 5) of N_0, *Z*, AAR, and also (new in this paper) the rate of change of AAR over time (d*AAR*/d*t*). Therefore, attempts to explain recruitment variations should consider the existence of temporal change in AAR. For spawning (N_0) variation to dominate in determining recruitment, it must exceed the variation in recruitment caused by AAR variation at the prevailing level of mortality, likewise for temporal variation in mortality.

The link of changes in AAR with changes in recruitment suggests how subtle changes in either abiotic or biotic environmental factors, which affect growth rate and AAR, can be amplified into recruitment surplus or failure. Thus they may help account for seasonally skewed recruitment of tropical species and the modal timing of life-history events within seasons in nontropical species.

The theory gives indirect access to parameters difficult to measure in the field: using the model (via simulation or via the modified Doppler equation) to construct predicted recruitment, observed recruitment can in principle be subtracted to give residuals. Residuals could be used to detect and, to some extent, describe temporal patterns not included in inputs to the model. For example, by elimination, if the temporal structure is adequately described in two of the three input variables (N_0, *Z*, or AAR), then the bulk of the unexplained (residual) temporal pattern would give insight to pattern in the less-known variable. The dynamics generated by temporal variation in AAR do not depend on sinusoidal or any particular pattern of temporal structure; any structure that can be described either

Fig. 9. Graphic estimation of recruitment peak timing from the AAR curve. Examples are for time-specific mortality low (B, ▲) or high (C, ●). Part A: AAR as in Fig. 7. Cardinal points CP1 and CP3 are maximum and minimum AAR (open circles), and CP2 and CP4 are the most negative and most positive dAAR/d*t* (open triangles). (B and C) Recruitment (as individuals per unit time) profiles from the HDR model using modified Doppler equation at $S = 1.0$ and $S = 0.7$. The long arrows angled downward from cardinal points are larval trajectories (lines with slope = –1), and their x values at $y = 0$ give timing (x value) of recruitment peaks and troughs. The derivatives (CP2 and CP4) are useful in predicting recruitment peaks at very low mortality, while the simple extremes of AAR (CP1 and CP3) are useful in predicting the peaks at high mortality. At intermediate survival rates the peak positions also will be intermediate but cannot readily be determined by geometry.

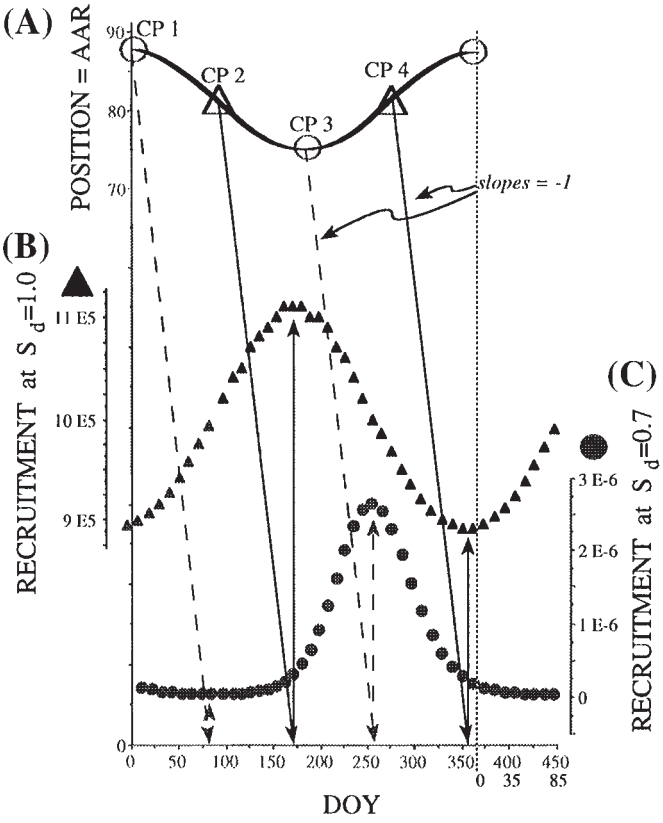

as a function, or even as a list, of AARs over time can be used in equations or simulation.

The logic presented in this paper is not limited to fish and applies to any definition of recruitment or to the duration of any stage, whether it coincides with a biological milestone (e.g., settlement, metamorphosis, germination, flowering, emergence, etc.) or not (e.g., size). The main limitation with many organisms may be the difficulty of determining AAR. Young fish record daily growth as incremental growth of otoliths, and many bivalves set down growth lines that can be used to determine age (e.g., Evans 1972), but in species without such growth-recording structures, individuals can sometimes be individually marked and followed to estimate the variability of time required to complete important life-history milestones.

Fig. 10. Comparing predictions using the modified Doppler equation (eq. 3; ▲) and the numerical simulation program (●). Panels A, B, and C compare modified Doppler and simulation results for $S = 1.0$, 0.9, and 0.6, respectively. Results are virtually identical. (However, although the match is excellent at the moderate AAR slopes here, caution is advised if curves contain high |dAAR/d*t*| (about 0.5 or more) because the accuracy of the modified Doppler equation may diminish.) Numerical simulation results were smoothed using a 28-point running mean, which introduces a lag of ~14 days relative to the results of the modified Doppler equation.

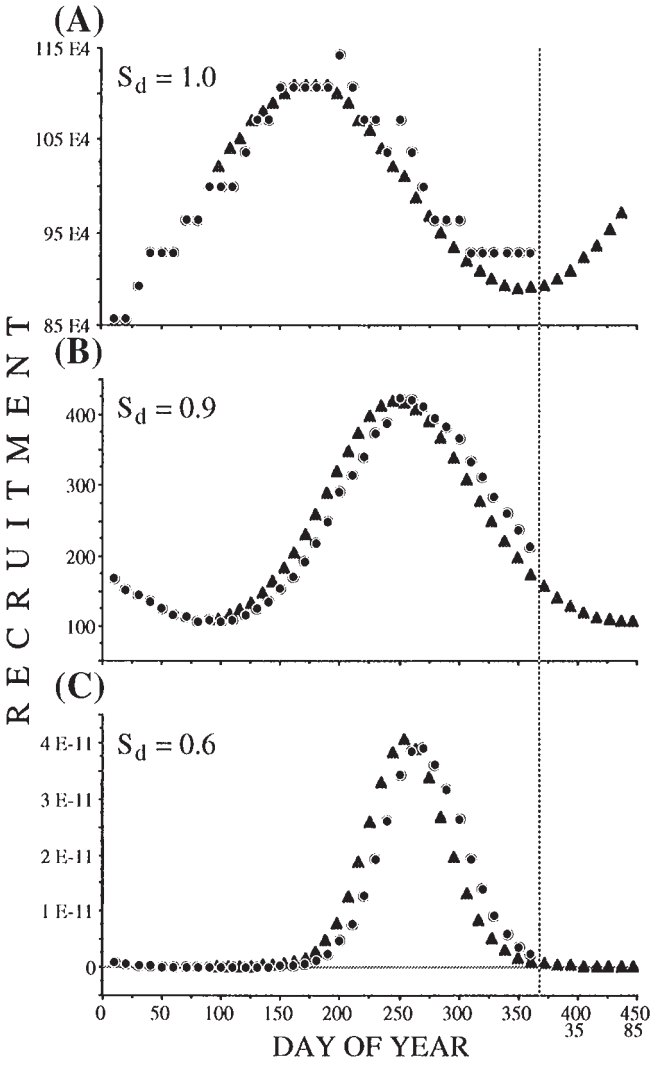

● Calculated by numerical simulation
▲ Calculated by Doppler equation

In fishes with seasonally restricted spawning periods, changes in AAR would still affect the similarity of the recruitment pattern to the production pattern. Failure to acknowledge AAR variation could prevent identification of the most important spawning periods. Lags from hatch to recruitment (AAR) should not be assumed constant (e.g., Robertson et al. 1988; Robertson 1990), because if this assumption is false, inference of peak spawning times from recruitment pattern will be unreliable.

On evolutionary time scales, an AAR curve that is stable (cycle-to-cycle) may select for preferential allocation of reproductive effort to certain seasons to take advantage of the AAR seasonal minimum. This is not equally physically possible among species: preferential allocation would be less expected in smaller fish owing to their higher annual total egg mass/body mass ratio (Burt et al. 1988). Long-term variations in the AAR cycle's mesor or its amplitude could reflect long-term climatic or environmental variation. Spawning at times or seasons other than at the AAR minimum may be selected for if competition at an over-subscribed AAR minimum diminishes its advantages, but a shorter AAR would still be an attractor according to its rank (fitness benefit) among other attractors (biotic or abiotic), which may be synchronous or not. In other words, AAR variation would consitute a part of the landscape of selective force that forms reproductive peaks, but it could be masked by, or could mask, others. The hypothesis of preferential allocation of reproductive effort toward the AAR minimum could be probed by looking for peaks in reproduction at times inconsistent with other variations that might influence reproduction directly (such as food availability and temperature) in the adult habitat, yet consistent with optimization of AAR in progeny.

Although it is mathematically unavoidable that AAR plays a large role in recruitment, generating 10- to a 100-fold variation at plausible time-specific survival rates, the importance of that role relative to other factors, which also may have large effects, remains a question. For *S. punctatum* (Fig. 1E), the resemblance of observed phase relationships (temporal locations of minima and maxima in AAR and yield) to model output (Fig. 7) supports seasonal shifts in AAR as being capable contributing greatly to observed seasonal recruitment variation. If other factors also contribute to the temporal structure of fishery variation they must either be small or nearly balance each other, because the predicted curves are already quite similar to the observed fishery. The relative contribution of other factors remains to be determined for *S. punctatum.*

Acknowledgements

With pleasure I acknowledge the Young Canadian Researchers Award (International Development Research Centre) for support of fieldwork; the cooperation of the Fisheries Division of the Commonwealth of Dominica, W.I.; the enthusiasm of John D. Archbold; a Fellowship from Memorial University of Newfoundland and assistance from Natural Sciences and Engineering Research Council grants to J.A. Brown; discussions with Pierre Pepin, Joe Brown, Ian McLaren, Peter Earle, and W.G. Warren; comments on the manuscript from M.C. Gomes, R. Hooper, P. Pepin, J.A. Brown, I.A. McLaren, B.X. Sanderson, E.R. Deutsch, and anonymous reviewers; encouragement of the Deorksen Institute; and the generous patience of my family.

References

Batschelet, E. 1981. Circular statistics in biology. Academic Press, London.

Bell, K.N.I. 1994. Life cycle, early life history, fisheries and recruitment dynamics of diadromous gobies of Dominica, W.I., emphasising *Sicydium punctatum* Perugia. Ph.D. thesis, Memorial University of Newfoundland, St. John's.

Bell, K.N.I., Pepin, P., and Brown, J.A. 1995. Seasonal, inverse cycling of length- and age-at-recruitment in the diadromous gobies *Sicydium punctatum* and *Sicydium antillarum* (Pisces) in Dominica, West Indies. Can. J. Fish. Aquat. Sci. **52**: 1535–1545.

Bliss, C.I. 1958. Periodic regression in biology and climatology. Bull. Conn. Agric. Exp. Stn. New Haven No. 615. pp. 1–55.

Burt, A., Kramer, D.L., Nakatsuru, K., and Spry, C. 1988. The tempo of reproduction in *Hyphessorbrycon pulchripinnis* (Characidae), with a discussion on the biology of 'multiple spawning' in fishes. Environ. Biol. Fishes, **22**: 15–27.

Chambers, R.C., and Leggett, W.C. 1987. Size and age at metamorphosis in marine fishes: an analysis of laboratory-reared winter flounder (*Pseudopleuronectes americanus*) with a review of variation in other species. Can. J. Fish. Aquat. Sci. **44**: 1936–1947.

Cowen, R.K. 1991. Variation in the planktonic larval duration of the temperate wrasse *Semicossyphus pulcher*. Mar. Ecol. Prog. Ser. **69**: 9–15.

Doppler, J.C. 1842. Ueber das Farbige Licht der Doppelsterne und einiger anderer Gestirne des Himmels. Abh. Konigl. Böhmischen Ges. Wiss. 5th Ser. 2: 465. (Not seen. Cited in Hujer, Karel, 1955, Sesquicentennial of Christian Doppler. Am. J. Phys. **23**: 51–54.)

Evans, J.W. 1972. Tidal growth increments in the cockle *Clinocardium nuttali*. Science (Washington, D.C.), **176**: 416–417.

Hoenig, J.M., Pepin, P., and Lawing, W.D. 1990. Estimating relative survival for two groups of larval fishes: do older larvae survive better than young? Fish. Bull. U.S. **88**: 485–491.

Houde, E.D. 1987. Fish early life dynamics and recruitment variability. Am. Fish. Soc. Symp. **2**: 17–29.

Markle, D.F., Harris, P.M., and Toole, C.L. 1992. Metamorphosis and an overview of early-life-history stages in Dover sole *Microstomus pacificus*. Fish. Bull. U.S. **90**: 285–301.

McCormick, M.I. 1994. Variability in age and size at settlement of the tropical goat fish *Upeneus tragula* (Mullidae) in the northern Great Barrier Reef lagoon. Mar. Ecol. Prog. Ser. **103**: 1–15.

Otten, E.W. 1992. Doppler effect. *In* McGraw-Hill encyclopedia of science and technology. Vol. 5. McGraw-Hill Inc., New York. pp. 396–399.

Pauly, D. 1985. Population dynamics of short-lived species, with emphasis on squids. NAFO Sci. Coun. Stud. **9**: 143–154.

Pauly, D. 1990. Length-converted catch curves and the seasonal growth of fishes. Fishbyte (Newsletter of Network of Tropical Fisheries Scientists), **3**: 33–38.

Pepin, P. 1989. Using growth histories to estimate larval fish mortality rates. Rapp. P.-V. Reun. Cons. Int. Explor Mer, **191**: 324–329.

Pepin, P. 1991. Effect of temperature and size on development, mortality, and survival rates of the pelagic early life history stages of marine fish. Can. J. Fish. Aquat. Sci. **48**: 503–518.

Peterman, R.M., and Bradford, M.J. 1987. Wind speed and mortality rate of a marine fish, the northern anchovy (*Engraulis mordax*). Science (Washington, D.C.), **235**: 354–356.

Pitcher, T.J., and MacDonald, P.D.M. 1973. Two models for seasonal growth in fishes. J. Appl. Ecol. **10**: 599–606.

Radtke, R.L., Kinzie, R.A., and Folsom, S.D. 1988. Age at recruitment of Hawaiian freshwater gobies. Environ. Biol. Fishes, **23**: 205–213.

Ricker, W.E. 1975. Computation and interpretation of biological statistics of fish populations. Bull. Fish. Res. Board Can. No. 191.

Robertson, D.R. 1990. Differences in the seasonalities of spawning and recruitment of some small neotropical reef fishes. J. Exp. Mar. Biol. Ecol. **144**: 49–62.

Robertson, D.R. 1992. Patterns of lunar settlement and early recruitment in Caribbean reef fishes at Panama. Mar. Biol. **114**: 527–537.

Robertson, D.R., Green, D.G., and Victor, B.C. 1988. Temporal coupling in the production and recruitment of larvae of a Caribbean reef fish. Ecology, **69**: 370–381.

Roughgarden, J., Gains, S., and Possingham, H. 1988. Recruitment dynamics in complex life cycles. Science (Washington, D.C.), **241**: 1460–1466.

Victor, B.C. 1982. Daily otolith increments and recruitment in two coral reef wrasses, *Thalassoma bifasciatum* and *Halichoeres bivittatus*. Mar. Biol. **71**: 203–208.

Victor, B.C. 1984. Coral reef fish larvae: patch size estimation and mixing in the plankton. Limnol. Oceanogr. **29**: 1116–1119.

Victor, B.C. 1986*a*. Delayed metamorphosis with reduced larval growth in a coral reef fish (*Thalassoma bifasciatum*). Can. J. Fish. Aquat. Sci. **43**: 1208–1213.

Victor, B.C. 1986*b*. Duration of the planktonic larval stage of one hundred species of Pacific and Atlantic wrasses (family Labridae). Mar. Biol. **90**: 317–326.

Wellington, G.M., and Victor, B.C. 1989. Planktonic larval duration of one hundred species of Pacific and Atlantic damselfishes (Pomacentridae). Mar. Biol. **101**: 557–567.

Wellington, G.M., and Victor, B.C. 1992. Regional differences in duration of the planktonic larval stage of reef fishes in the eastern Pacific Ocean. Mar. Biol. **113**: 491–498.

Werner, E.E., and Gilliam, J.F. 1984. The ontogenetic niche and species interactions in size-structured populations. Annu. Rev. Ecol. Syst. **15**: 393–425.